

AD-A166 668

ON THE ELECTRODEPOSITION AND CHARACTERIZATION OF  
NIOBIUM FROM FUSED FLUOR (U) ARMY ARMAMENT RESEARCH  
AND DEVELOPMENT CENTER WATERVLIET NY C.

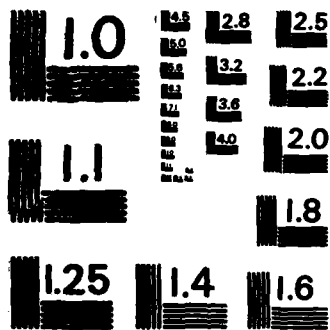
1/1

UNCLASSIFIED

G P CAPSIMALIS ET AL FEB 86 ARCCB-TR-86008 F/G 13/8

NL





MICROCOPY RESOLUTION TEST CHART  
NATIONAL BUREAU OF STANDARDS-1963-A

12

AD E440323

TECHNICAL REPORT ARCCB-TR-86008

**ON THE ELECTRODEPOSITION AND CHARACTERIZATION  
OF NIOBIUM FROM FUSED FLUORIDE ELECTROLYTES**

AD-A166 668

G. P. CAPSIMALIS  
E. S. CHEN  
R.E. PETERSON  
I. AHMAD

DTIC  
ELECTE  
MAR 19 1986  
S D

FEBRUARY 1986



**US ARMY ARMAMENT RESEARCH AND DEVELOPMENT CENTER  
CLOSE COMBAT ARMAMENTS CENTER  
BENET WEAPONS LABORATORY  
WATERVLIET, N.Y. 12189-4050**

DTIC FILE COPY

APPROVED FOR PUBLIC RELEASE; DISTRIBUTION UNLIMITED

86 3 19 007

#### DISCLAIMER

The findings in this report are not to be construed as an official Department of the Army position unless so designated by other authorized documents.

The use of trade name(s) and/or manufacturer(s) does not constitute an official indorsement or approval.

#### DESTRUCTION NOTICE

For classified documents, follow the procedures in DoD 5200.22-M, Industrial Security Manual, Section II-19 or DoD 5200.1-R, Information Security Program Regulation, Chapter IX.

For unclassified, limited documents, destroy by any method that will prevent disclosure of contents or reconstruction of the document.

For unclassified, unlimited documents, destroy when the report is no longer needed. Do not return it to the originator.

REPORT DOCUMENTATION PAGE		READ INSTRUCTIONS BEFORE COMPLETING FORM
1. REPORT NUMBER ARCCB-TR-86008	2. GOVT ACCESSION NO. AD-A166668	3. RECIPIENT'S CATALOG NUMBER
4. TITLE (and Subtitle) ON THE ELECTRODEPOSITION AND CHARACTERIZATION OF NIOBIUM FROM FUSED FLUORIDE ELECTROLYTES		5. TYPE OF REPORT & PERIOD COVERED Final
		6. PERFORMING ORG. REPORT NUMBER
7. AUTHOR(s) G. P. Capsimalis, E. S. Chen, R. E. Peterson, and I. Ahmad (See Reverse)		8. CONTRACT OR GRANT NUMBER(s)
9. PERFORMING ORGANIZATION NAME AND ADDRESS US Army Armament Research & Development Center Benet Weapons Laboratory, SMCAR-CCB-TL Watervliet, NY 12189-4050		10. PROGRAM ELEMENT, PROJECT, TASK AREA & WORK UNIT NUMBERS AMCMS No. 6111.02.H600.011 PRON No. 1A52F51D1A1A
11. CONTROLLING OFFICE NAME AND ADDRESS US Army Armament Research & Development Center Close Combat Armaments Center Dover, NJ 07801-5001		12. REPORT DATE February 1986
		13. NUMBER OF PAGES 17
14. MONITORING AGENCY NAME & ADDRESS (if different from Controlling Office)		15. SECURITY CLASS. (of this report) Unclassified
		15a. DECLASSIFICATION/DOWNGRADING SCHEDULE
16. DISTRIBUTION STATEMENT (of this Report) Approved for Public Release; Distribution Unlimited		
17. DISTRIBUTION STATEMENT (of the abstract entered in Block 20, if different from Report)		
18. SUPPLEMENTARY NOTES		
19. KEY WORDS (Continue on reverse side if necessary and identify by block number) Electrodeposition Molten Salt Refractory Coatings High Temperature Resistant Erosion Material Microstructure Characterization		
20. ABSTRACT (Continue on reverse side if necessary and identify by block number) The electrodeposition of niobium from a binary electrolyte consisting of KF and NaF was characterized and compared with the ternary electrolyte of LiF, NaF, and KF. The deposition experiments were conducted at current densities between 5 and 35 mA/cm <sup>2</sup> and electrolyte temperatures between 725° and 800°C. DTA measurements indicated the melting points to be 450° and 710°C for the ternary and binary electrolytes with added K <sub>2</sub> NbF <sub>7</sub> ; however, it was necessary (CONT'D ON REVERSE)		

7. AUTHORS (CONT'D)

I. Ahmad  
U.S. Army Reserach, Development, and Standardization Group  
London, England

20. ABSTRACT (CONT'D)

to operate both electrolytes above 725°C to obtain dense coherent deposits. Coating morphology was described by optical and scanning electron microscopy (SEM) morphology, while coating structure and properties were characterized by x-ray diffraction analysis. In particular, a series of diffraction measurements were reported to describe the changes in the microstructure of the deposited material as a function of the preparation conditions.

**TABLE OF CONTENTS**

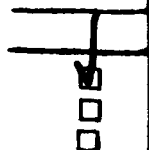
	<u>Page</u>
<b>ACKNOWLEDGEMENTS</b>	11
<b>INTRODUCTION</b>	1
<b>EXPERIMENTAL PROCEDURE</b>	1
<b>RESULTS AND DISCUSSION</b>	3
<b>CONCLUSION</b>	7
<b>REFERENCES</b>	8

**TABLES**

1. TEXTURE COEFFICIENTS	4
-------------------------	---

**LIST OF ILLUSTRATIONS**

1. Diagram of electroplating cell.	9
2. Variation of cathode efficiency with current density for the electrodeposition of niobium from LiF-NaF-KF + K <sub>2</sub> NbF <sub>7</sub> at 725°C, 750°C, 775°C, and 800°C.	10
3. Variation of cathode efficiency with current density for the electrodeposition of niobium from KF-NaF + K <sub>2</sub> NbF <sub>7</sub> at 750°C, 775°C, 800°C, and 875°C.	11
4. Microstructure of niobium plated at 775°C from LiF-NaF-KF + K <sub>2</sub> NbF <sub>7</sub> .	12
5. Microstructure of niobium plated at 750°C from NaF-KF + K <sub>2</sub> NbF <sub>7</sub> .	13
6. SEM of niobium surface and x-ray reflections.	14
7. Microstructure of niobium plated at 775°C from LiF-NaF-KF + K <sub>2</sub> NbF <sub>7</sub> + 10 w/o K <sub>2</sub> TaF <sub>7</sub> .	15
8. Microstructure of niobium plated at 750°C from NaF-KF + K <sub>2</sub> NbF <sub>7</sub> + 10 w/o NaBF <sub>4</sub> .	15



J. ...	
By _____	
Distribution _____	
<b>Availability Codes</b>	
Dist	Avail and/or Special
<b>A-1</b>	

## ACKNOWLEDGEMENTS

The authors are greatly indebted to the support work provided by Chris Rickard and Leo McNamara. These two individuals were invaluable for their aid and expertise in the fields of metallography and scanning electron microscopy.

## INTRODUCTION

The electrodeposition of refractory metal coatings from molten salts appears to be a promising surface-finishing method for protecting metals against corrosion and high temperature oxidation. Currently, a number of melts are available for plating a variety of metals including tantalum, niobium, molybdenum, zirconium, and tungsten (refs 1-4). Of these metals, niobium is one of the most widely investigated (refs 5-9), and appears to have the potential to be developed for ordnance applications. In this regard, strength, low stress, and high hardness are additional properties needed to withstand both corrosion and erosion environments. In this study a comparative investigation is made of the effects of temperature, current density, and additives on the electrodeposition of niobium from the fused salt systems  $\text{KF-NaF}$  and  $\text{LiF-NaF-KF}$  (FLINAK). The morphology and structure of the deposits were characterized both metallographically and by SEM and x-ray diffraction.

## EXPERIMENTAL PROCEDURE

The solvents used consisted of (1) a binary eutectic mixture of  $\text{NaF-KF}$ , and (2) a ternary eutectic mixture of  $\text{KlF-NaF-KF}$  prepared from reagent grade chemicals. The procedure for preparing the fused niobium electrolytes involved the addition of 3.2 w/o  $\text{K}_2\text{NbF}_7$  to the binary eutectic, 2.5 w/o to the ternary eutectic, and outgassing the mixture under vacuum at  $400^\circ\text{C}$  for one week to remove adsorbed moisture. The dried mixtures were fused in nickel crucibles in an argon atmosphere. Purification consisted of prolonged

---

References are listed at the end of this report.

electrolysis until fairly consistent cathode efficiencies were obtained. The plating of niobium alloys containing chromium or boron was conducted by adding  $K_2CrF_6$ , up to 5.0 w/o percent, and  $NaBF_4$  at 10 w/o percent to  $KF-NaF$ . Niobium-tantalum alloy plating was also investigated by adding up to 12.5 w/o percent  $K_2TaF_7$  to FLINAK.

A diagram of the electrochemical cell used in this study is shown schematically in Figure 1. The reactor container was constructed from 316 stainless steel and heated with a single-zone Mellor furnace. A proportional controller was used to regulate the furnace temperature. Metallurgical grade niobium and OFHC copper plates with an immersed area of 1.8 by 2.5 cm were used as electrodes. To monitor the temperature of the fused electrolyte, a platinum/platinum rhodium thermocouple housed in a closed-end nickel tube was used.

The x-ray study used an approach similar to the method of inverse pole figures to determine the texture coefficients of the deposited coatings. The calculated texture coefficients provided a good representation of the fiber texture normal to the deposition plane of the sample. A Philips x-ray diffractometer was employed to scan each sample for the various x-ray intensity peaks in the  $2\theta$  ranges of  $0^\circ$  to  $76.00^\circ$ .  $MoK_\alpha$  radiation ( $\lambda = 0.70926\text{\AA}$ ) was monochromatized by means of an LiF curved crystal. The x-ray generator was operated at 45KV and 15 mA. A one-degree divergence of the incident beam was maintained by a  $2\theta$  compensating slit, while the receiving slit was set at  $0.2^\circ$ . The signal from the counter for each step was sent to the computer where the intensity of each  $0.02^\circ$   $2\theta$  step was recorded and the various x-ray corrections were applied. By summation, the integrated

intensity of each x-ray peak determined the relative integrated intensities or texture coefficients for each peak calculated by:

$$T_c(hkl) = \frac{I(hkl)/I^\circ(hkl)}{\frac{1}{N} \sum_{i=1}^N I_i(hkl)/I_i^\circ(hkl)} \quad (1)$$

where  $I(hkl)$  is the integrated intensity from an hkl peak, and  $I^\circ(hkl)$  is the integrated intensity from the same hkl peak obtained from a powder sample which had random texture. A FORTRAN program was written for a VAX 11/730 to control the experiment and is available from the authors. Using this program, the data for Table I was obtained using samples from the various deposition conditions.

#### RESULTS AND DISCUSSION

The relationship between current efficiency and current density is shown in Figure 2 for the electrodeposition of niobium from the FLINAK system. At 725°C, the efficiency increases substantially with an increase in current density. At 750° and 775°C, the increase is inefficient and at 800°C the efficiency decreases as the current density is raised. Figure 2 also shows that the efficiency decreases progressively with increasing temperature for constant current density. This result is attributed to an acceleration at high temperatures of the disproportionation reaction involving  $NbF_7^-$  and  $NbF$  to form  $Nb^{+4}$  and effectively reduces the concentration of  $NbF$  for reduction to metal. A similar argument was used by Senderoff (ref 2) in his explanation of the observed decrease in efficiency at low current densities for the FLINAK system.

TABLE I. TEXTURE COEFFICIENTS

DATE TEMP NUMBER °C	SAMPLE NUMBER	CURRENT DENSITY	E P L E C T I O N S			I - R A Y			E K L			E P P I - H A R D - C I E N C Y M E S S								
			220	211	200	211	220	211	200	211	220		211	200						
1	725	36	2.1	6.3	1.8	3.2	0.7	824	111	850	99	20.0	6.5	0.0	10.0	1.6	0.3	0.0	540	
			0.5	9.3	0.9	0.4	10.0	824	111	98	21.0	7.5	0.0	0.0	10.0	1.6	0.3	2.5	500	
			0.1	3.5	0.1	0.0	10.0	1050	124	875	100	20.0	8.0	0.0	0.1	10.0	1.9	0.4	0.5	610
			0.0	0.6	1.9	4.1	0.0	794	109	101	20.0	10.0	0.0	0.0	0.0	10.0	2.7	0.0	0.0	145
			0.0	0.3	1.9	2.2	0.0	824	-	102	20.0	6.0	0.0	0.0	0.4	10.0	2.2	0.6	2.2	146
2	750	34	0.0	0.6	1.9	0.1	0.0	824	-	90	20.0	10.0	0.0	0.0	1.6	2.5	0.0	0.0	540	
			0.0	0.3	0.0	0.0	0.0	824	-	92	22.0	8.0	0.0	0.0	0.0	2.7	0.5	1.6	610	
			0.0	0.6	1.7	0.0	0.0	744	-	108	15.0	0.0	0.0	0.0	0.0	0.0	0.0	0.0	-	
			0.0	2.8	0.0	0.1	0.0	834	-	107	23.0	6.5	0.0	0.0	0.0	0.0	0.0	0.0	0.0	320
			0.0	2.5	1.8	0.0	1.2	804	110	126	32.0	6.1	10.0	1.7	1.3	5.4	0.0	0.0	0.0	750
3	775	24	0.0	1.8	1.8	0.9	0.0	784	89	128	55.0	1.5	10.0	0.5	0.1	2.5	0.0	0.0	0.0	
			0.0	0.6	2.4	0.4	0.0	804	-	129	75.0	0.4	10.0	0.6	0.0	1.0	0.0	0.0	0.0	
			0.0	0.3	1.9	4.9	0.0	764	96	127	39.0	3.4	10.0	1.3	0.0	0.0	0.0	0.0	0.0	
			0.0	3.9	1.9	0.0	0.0	764	111	128	55.0	1.5	10.0	0.5	0.1	2.5	0.0	0.0	0.0	
			0.0	1.4	2.3	1.7	0.4	864	102	130	93.0	0.3	10.0	0.4	0.0	0.0	0.0	0.0	0.0	0.0
4	800	33	0.0	5.7	2.3	2.3	0.0	734	113	850	111	25.0	2.5	10.0	2.2	0.6	5.3	0.0	345	
			0.0	1.6	2.3	0.5	0.0	664	115	120	30.0	4.3	10.0	5.5	1.9	9.0	0.0	0.0	890	
			0.0	2.4	0.3	0.8	0.0	634	119	121	32.0	2.7	10.0	2.8	0.7	6.0	0.1	0.0	850	
			0.0	10.0	0.4	0.1	3.8	604	-	113	34.0	3.0	10.0	2.5	1.0	2.2	0.1	0.0	780	
			0.0	10.0	0.7	0.0	0.0	634	119	138	27.0	10.0	0.0	0.0	0.0	0.0	0.0	0.0	500	
5	750	63	10.0	2.4	0.3	0.8	0.0	604	-	139	22.0	1.9	0.1	5.9	2.4	0.3	0.0	1.2	760	
			0.0	10.0	0.4	0.1	3.8	604	-	140	21.0	3.6	0.7	10.0	0.9	0.2	3.6	0.0	800	
			0.0	10.0	0.7	0.2	3.1	644	-	145	18.0	0.0	10.0	0.0	0.0	0.0	0.0	0.0	500	
			0.0	3.9	0.6	10.0	0.1	774	-	142	22.0	0.0	10.0	0.0	0.0	0.0	0.0	0.0	710	
			0.0	10.0	1.2	0.6	8.7	794	-	143	23.0	0.0	10.0	0.0	0.0	0.0	0.0	0.0	0.0	740
6	775	58	0.0	10.0	0.0	0.9	0.0	774	-	144	26.0	0.0	10.0	0.0	0.0	0.0	0.0	0.0	750	
			0.0	10.0	0.4	4.0	0.0	704	-	148	15.0	0.0	10.0	0.0	0.0	0.0	0.0	0.0	620	
			0.0	1.3	1.8	10.0	0.0	704	-	147	23.0	0.0	10.0	0.0	0.0	0.0	0.0	0.0	670	
			0.0	10.0	1.7	1.1	1.6	714	-	151	29.0	1.9	10.0	0.4	0.3	0.7	0.0	0.0	700	
			0.0	5.9	2.5	0.3	0.5	724	-	149	32.0	0.0	10.0	0.0	0.0	0.0	0.0	0.0	0.0	820
7	800	67	0.0	10.0	1.4	1.1	2.2	734	-	150	37.0	0.1	10.0	0.0	0.0	0.0	0.0	0.0	860	
			0.0	10.0	0.0	0.2	0.1	504	-	157	16.0	0.4	10.0	0.1	0.0	0.0	0.0	0.0	780	
			0.0	2.5	1.7	2.0	0.2	604	-	154	24.0	0.0	10.0	0.0	0.0	0.0	0.0	0.0	750	
			0.0	1.7	2.0	0.1	0.0	624	125	153	30.0	0.0	10.0	0.0	0.0	0.0	0.0	0.0	790	
			0.0	4.7	2.8	0.1	0.0	674	132	155	30.0	0.0	10.0	0.0	0.0	0.0	0.0	0.0	820	
8	800	91	0.0	10.0	0.1	0.0	0.0	744	-	156	23.0	1.2	10.0	0.0	0.0	0.0	0.0	0.0	830	
			0.0	7.1	1.5	0.9	0.6	-	141	108	11.2	10.0	0.0	0.0	0.0	0.0	0.0	0.0	820	
			0.0	10.0	0.1	2.1	1.1	-	630	-	156	23.0	1.2	10.0	0.0	0.0	0.0	0.0	830	
			0.0	10.0	1.4	1.4	4.6	-	-	-	-	-	-	-	-	-	-	-	-	-
			0.0	2.6	0.4	0.4	4.6	-	-	-	-	-	-	-	-	-	-	-	-	-

1 - denotes 2 w/o  $K_2TaF_7$   
 2 - denotes 5 w/o  $K_2TaF_7$   
 3 - denotes 7.5 w/o  $K_2TaF_7$   
 4 - denotes 10 w/o  $K_2TaF_7$   
 5 - denotes 12.5 w/o  $K_2TaF_7$ , both results omitted from table.  
 1 = FLUOR +  $K_2TaF_7$   
 2 = BIRNBY +  $K_2TaF_7$   
 3 = BIRNBY MIX + 5 w/o  $K_2TaF_7$   
 4 = BIRNBY MIX + 10 w/o  $K_2TaF_7$   
 5 = FLUOR +  $K_2TaF_7$  +  $K_2TaF_7$

By comparison, the variation of efficiency for the binary eutectic, Figure 3, is more complex. For all temperatures concerned, the efficiency was seen to increase with current density, to pass through a maximum between 25 and 30 mA/cm<sup>2</sup>, and then to drop off at higher current densities. While the origin of the maximum is uncertain, a trend was established relating the plating efficiencies to the ratio of anode weight loss to cathode weight gain (A/C). The spread of A/C varied from near unity to 2.5. Higher efficiencies were associated with A/C values approaching unity and lower efficiencies associated for A/C values approaching 2.5. The significance of a high A/C ratio is that a larger number of NbF<sub>7</sub><sup>-</sup> ions are present during the electro-dissolution of the anode and consequently, the formation of niobium metal at the cathods is restricted once more by an enhancement of the disproportionation reaction.

The grain size of niobium deposits prepared from both types of electrolytes is influenced by current density. Figure 4 illustrates that some grain refinement was obtained by increasing the current density from 10 to 40 mA/cm<sup>2</sup> in the plating of niobium from FLINAK. Figure 5 shows a similar trend in grain refinement for the plating of niobium from NaF-KF. However, the slight refinement in grain size is not reflected in deposit hardness. In general, hardness values for deposits associated with FLINAK vary between 102 and 124 KHN while deposits produced from KF-NaF vary between 119 and 144 KHN.

The introduction of cationic additions to molten salt electrolytes produced interesting changes in deposit morphology and orientation. Tantalum added as K<sub>2</sub>TaF<sub>7</sub> in the range of 5 to 10 w/o produced bright niobium deposits from the FLINAK bath. Above and below this concentration, the deposit

structure and surface features appear similar to those plated without tantalum additions. It is interesting to note that these changes occur in the absence of tantalum codeposition. In all cases, analyses using an electron microprobe verified the absence of tantalum in the deposits. Sample 153 of Table I is a typical bright deposit plated from a FLINAK electrolyte containing 10 w/o percent  $K_2TaF_7$ . Its surface texture can be seen in Figure 6D and its microstructure consisting of fine columnar grains is seen in Figure 7. These features may be compared with deposits prepared without tantalum addition in Figures 4 (sample 26) and 6A. It was observed that bright deposits were obtained only in samples showing pure [100] orientation, i.e., sample numbers 142, 143, and 153. Brightness in the deposits gradually diminished with the appearance of mixed orientation. The orientation in deposits prepared without tantalum additions was notably different. At 725°C the deposits started with a [211] texture and as the current density increased from 18 mA to 42 mA, the texture changed to [111]. When the bath was increased to 750°C, the texture of the deposit became predominantly [110], and remained so as the temperature was increased to 775°. As the bath reached 800°C, the deposit was almost random at low current densities and some [110] texture developed as the current density was increased to 50 mA.

The addition of  $K_3CrF_6$  up to 5 w/o percent produced no observable differences in the morphology, orientation, or physical properties of niobium deposits produced from the NaF-KF bath. However, the addition of 10 w/o percent  $NaBF_4$  (sample number 126) markedly altered the growth orientation, surface texture (Figure 6C), and microstructure (Figure 8). While the presence of boron in the niobium deposits was verified, quantitative

evaluations were not made. Figures 6B and 6C show a comparison of the surface features of niobium deposits plated with and in the absence of boron addition.

The formation of deposit texture is dependent on boron incorporation as well. In this case, a [110] texture is predominant and, depending upon the temperature and current density, some [310] orientation emerges from the formation of a duplex texture. In the absence of boron additions, the binary bath cannot be adequately characterized by a single texture. At the lower temperature of 750°C the [211] texture is predominant. At 775°C no dominant trend in the formation of texture is observed. At 800°C a combination of samples with [110] and random orientation is obtained. At 875°C a [310] orientation becomes mixed with a [211] orientation to form a duplex type texture.

#### CONCLUSION

Observations have been made on the effects of temperature, current density, additions of  $K_3CrF_4$  and  $K_2TaF_7$  on the structure, and efficiency of the niobium deposits. Maxima were found in the plots of current efficiency versus current density for the KF-NaF solvent system, while linear relationships were obtained for FLINAK. The effect of various additives resulted in improvements in surface finish, grain size, and hardness. Although some correlation was observed between the texture and other properties studied, no attempt was made to study the growth mechanisms during electrocrystallization. Finally, it has been shown that the addition of tantalum and boron to the electrolyte produced deposits with improved properties.

#### REFERENCES

1. S. Senderoff and G. W. Mellors, Science, Vol. 153, 1966, p. 1495.
2. S. Senderoff, Metall. Revs., Vol. 11, 1966, p. 97.
3. D. Inman and S. H. White, Proceedings of the International Symposium on Molten Salt Electrolysis in Metal Production, Genoble, IMM, 1977, pp. 51-61.
4. D. Inman, Proceedings of the European Conference on Development of Molten Salts Applications, Geneva, Battelle, 1973, pp. 58-61.
5. G. W. Mellors and S. Senderoff, J. Electrochem. Soc., Vol. 112, 1965, p. 266.
6. G. W. Mellors and S. Senderoff, Plating, Vol. 51, October 1964, p. 972.
7. C. Decroly, A. Mukhtar, and R. Winand, J. Electrochem. Soc., Vol. 115, 1968, p. 905.
8. V. Cohen, J. Electrochem Soc., Vol. 128, 1981, p. 731.
9. T. Yoko and R. A. Bailey, Proceedings of the First International Symposium on Molten Salt Chemistry and Technology, Kyoto, Japan, 1983, pp. 111-114.

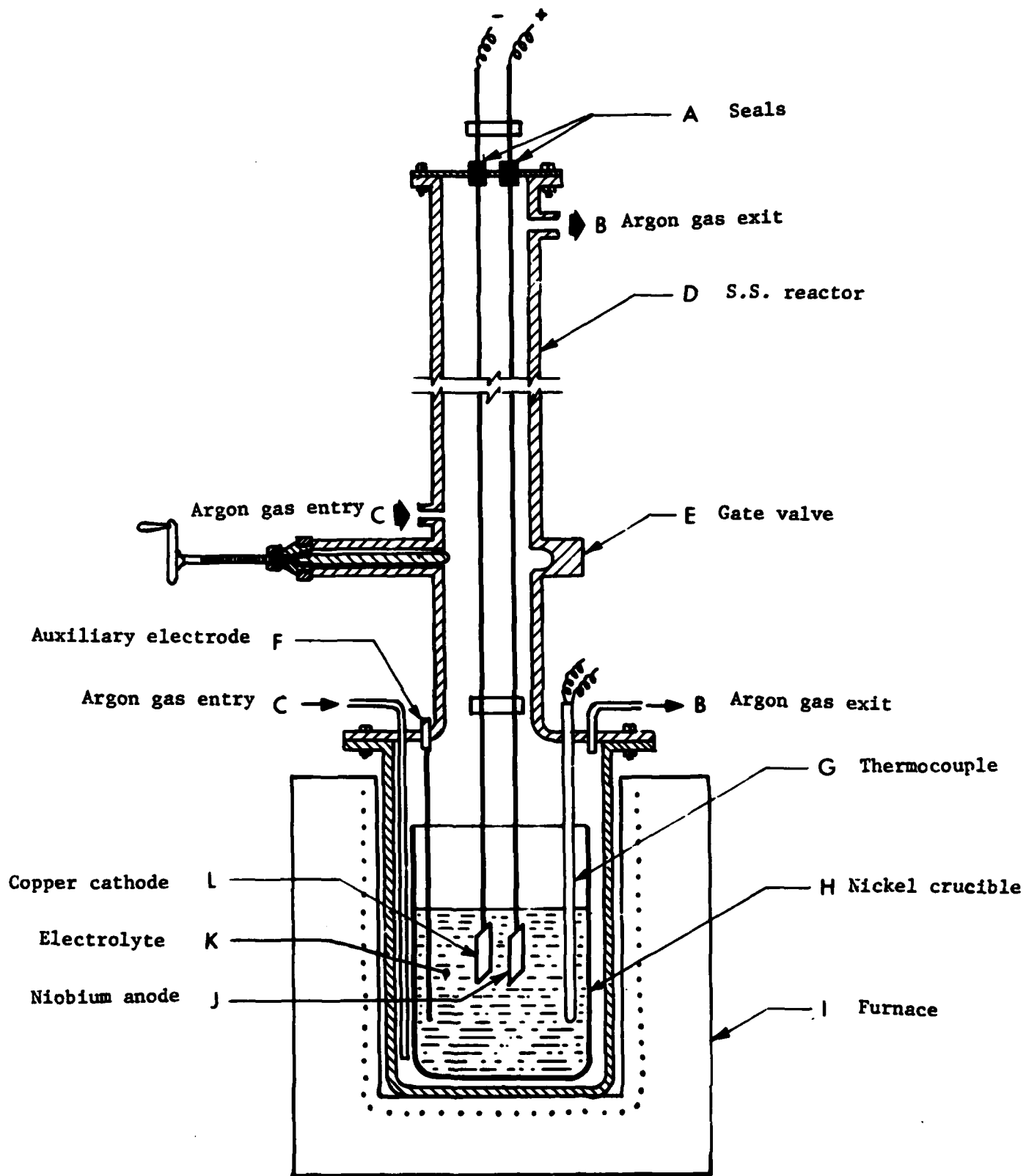


Figure 1. Diagram of electroplating cell.

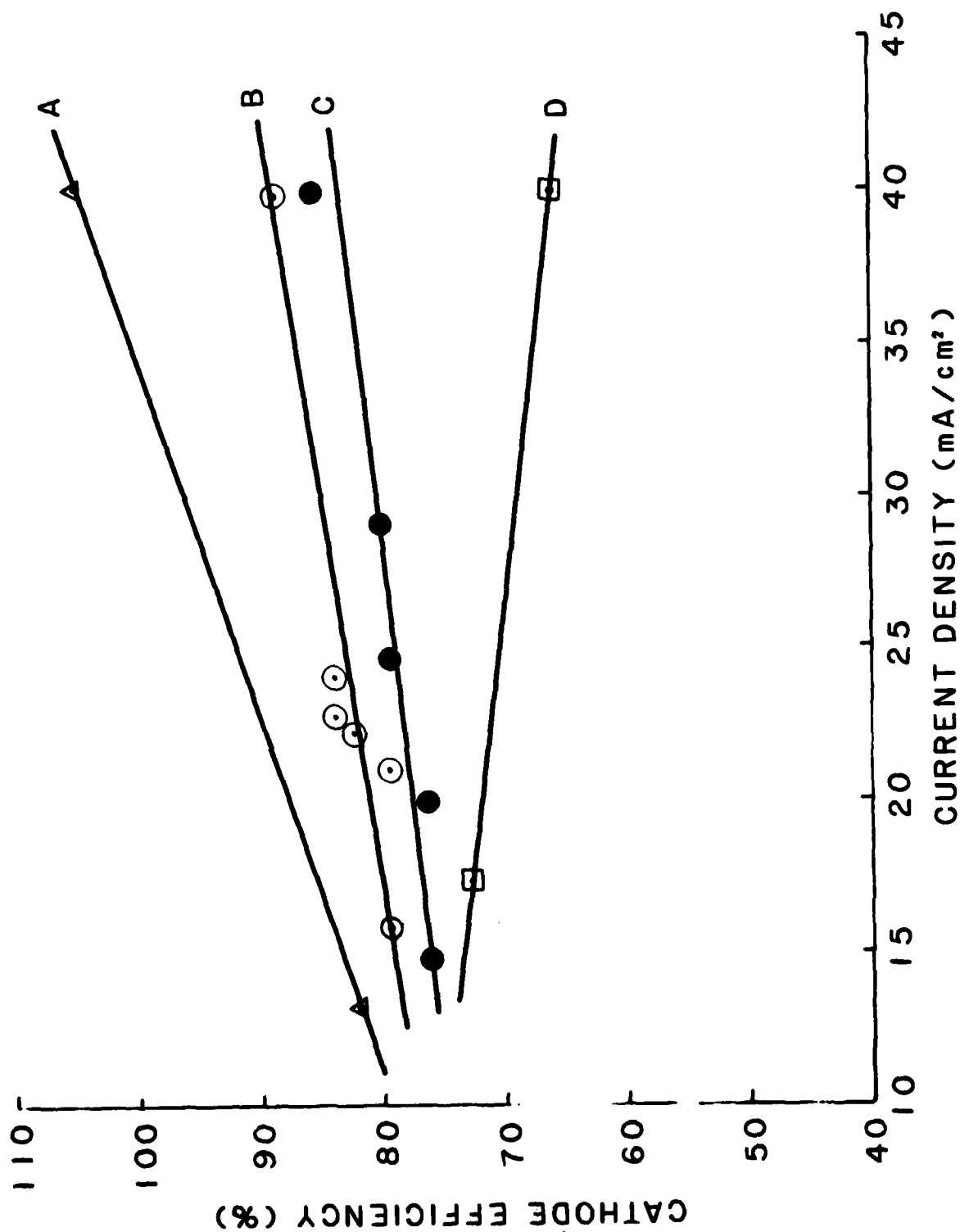


Figure 2. Variation of cathode efficiency with current density for the electrodeposition of niobium from  $\text{LiF-NaF-KF} + \text{K}_2\text{NbF}_7$  at  $725^\circ\text{C}$  (A),  $750^\circ\text{C}$  (B),  $775^\circ$  (C), and  $800^\circ\text{C}$  (D). Efficiency based on a four electron change in oxidation state.

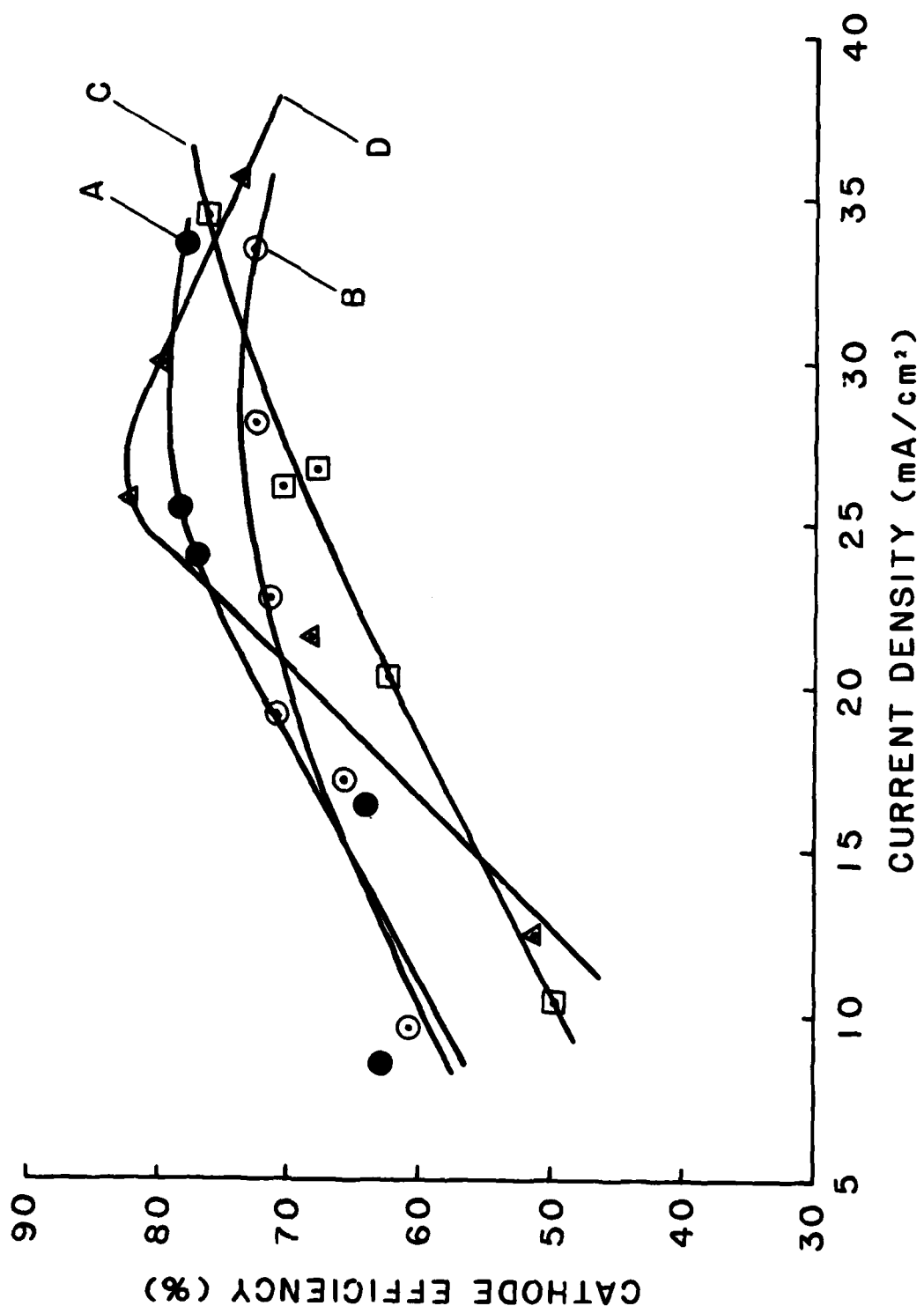
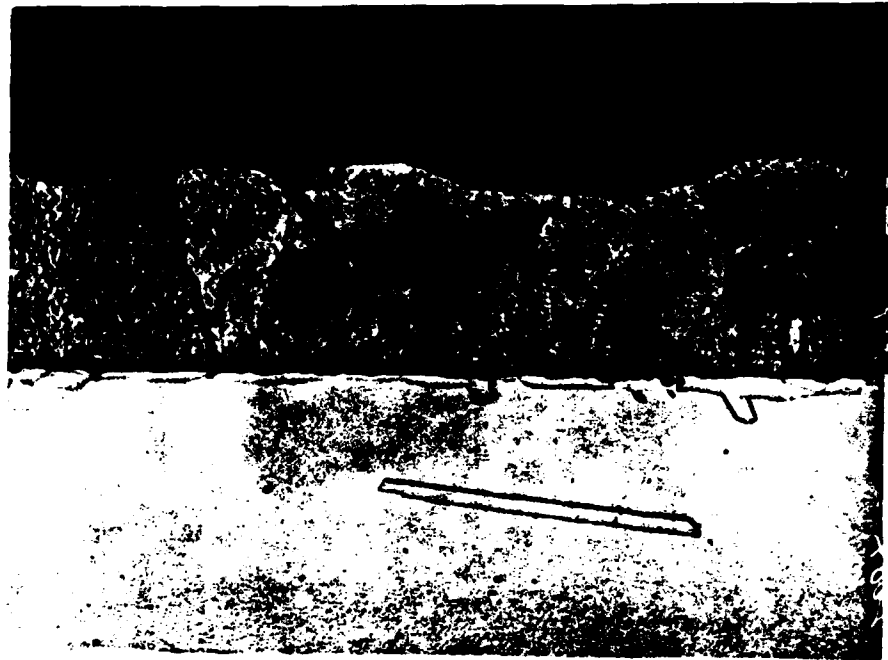


Figure 3. Variation of cathode efficiency with current density for the electrodeposition of niobium from  $\text{KF-NaF} + \text{K}_2\text{NbF}_7$  at  $750^\circ\text{C}$  (A),  $775^\circ\text{C}$  (B),  $800^\circ\text{C}$  (C), and  $875^\circ\text{C}$  (D). Efficiency based on a four electron change in oxidation state.



A

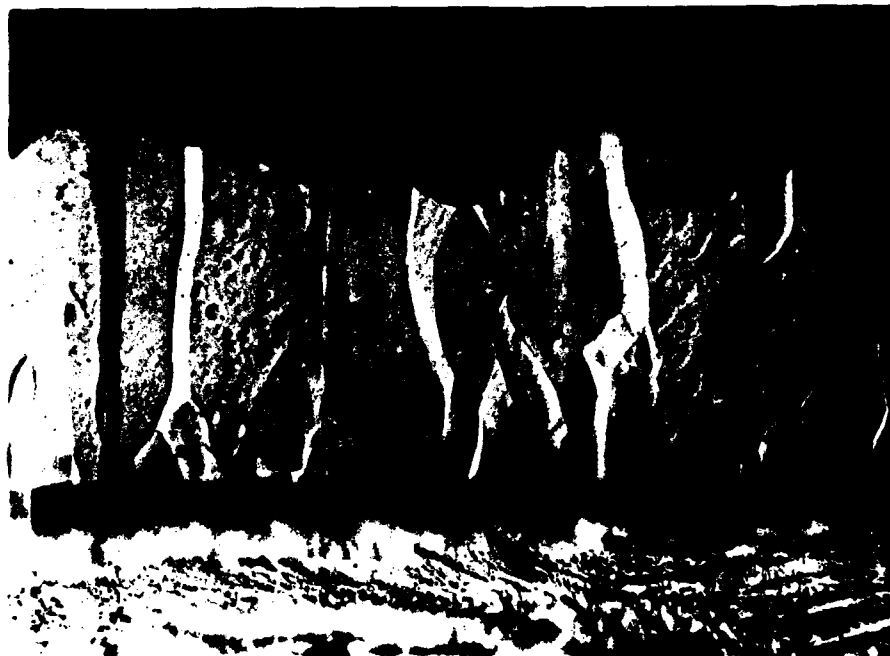


B

Figure 4. Microstructure of niobium plated at 775°C from  $\text{LiF-NaF-KF} + \text{K}_2\text{NbF}_7$ .  
A - 10  $\text{mA/cm}^2$ ; B - 40  $\text{mA/cm}^2$  (200X).



A



B

Figure 5. Microstructure of niobium plated at 750°C from NaF-KF + K<sub>2</sub>NbF<sub>7</sub>.  
A - 8.5 mA/cm<sup>2</sup>; B - 33.7 mA/cm<sup>2</sup> (500X).

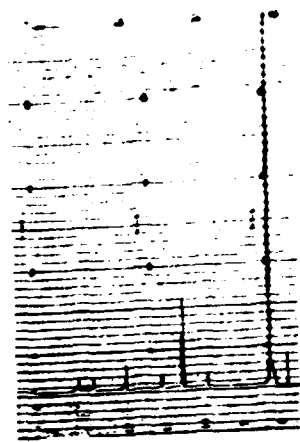
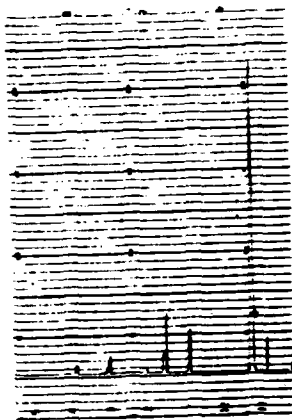
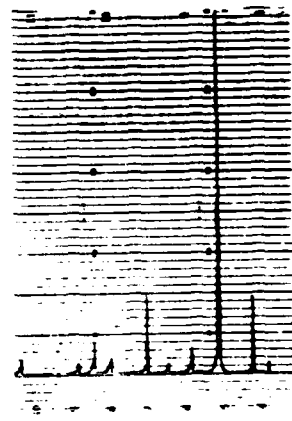
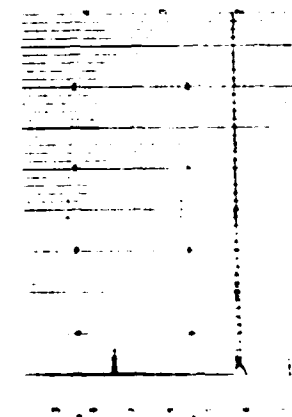
**A****B****C****D**

Figure 6. SEM of niobium surface and x-ray reflections. A -  $\text{LiF-NaF-KF} + \text{K}_2\text{NbF}_7$ ; B -  $\text{NaF-KF} + \text{K}_2\text{NbF}_7$ ; C -  $\text{NaF-KF} + \text{K}_2\text{NbF}_7 + 10 \text{ w/o NaBF}_4$ ; D -  $\text{LiF-NaF-KF} + \text{K}_2\text{NbF}_7 + 10 \text{ w/o K}_2\text{TaF}_7$ . Surface view (20X); SEM (1000X).

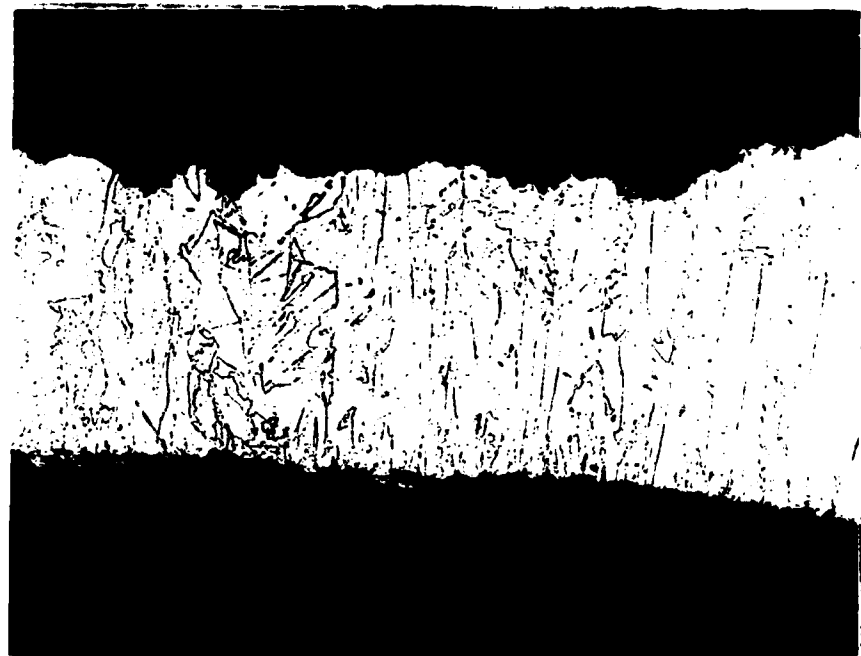


Figure 7. Microstructure of niobium plated at 775°C from LiF-NaF-KF + K<sub>2</sub>NbF<sub>7</sub> + 10 w/o K<sub>2</sub>TaF<sub>7</sub> (200X).

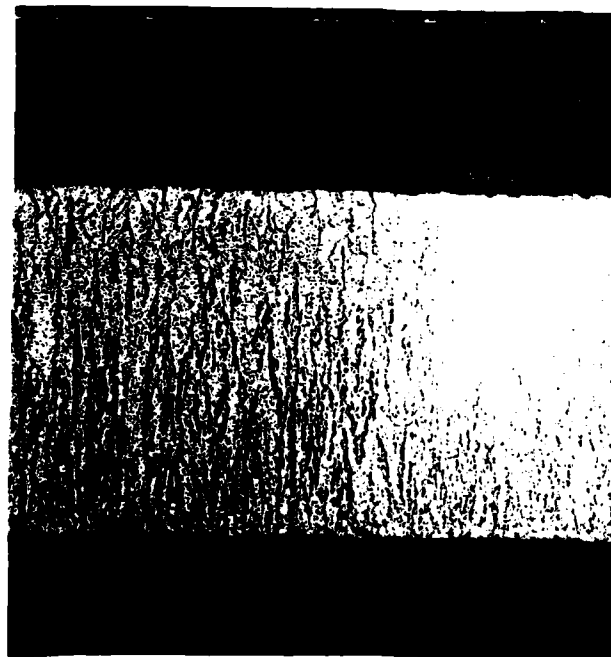


Figure 8. Microstructure of niobium plated at 750°C from NaF-KF + K<sub>2</sub>NbF<sub>7</sub> + 10 w/o NaBF<sub>4</sub> (200X).

TECHNICAL REPORT INTERNAL DISTRIBUTION LIST

	<u>NO. OF COPIES</u>
CHIEF, DEVELOPMENT ENGINEERING BRANCH	
ATTN: SMCAR-CCB-D	1
-DA	1
-DP	1
-DR	1
-DS (SYSTEMS)	1
-DS (ICAS GROUP)	1
-DC	1
-DM	1
 CHIEF, ENGINEERING SUPPORT BRANCH	
ATTN: SMCAR-CCB-S	1
-SE	1
 CHIEF, RESEARCH BRANCH	
ATTN: SMCAR-CCB-R	2
-R (ELLEN FOGARTY)	1
-RA	1
-RM	1
-RP	1
-RT	1
 TECHNICAL LIBRARY	5
ATTN: SMCAR-CCB-TL	
 TECHNICAL PUBLICATIONS & EDITING UNIT	2
ATTN: SMCAR-CCB-TL	
 DIRECTOR, OPERATIONS DIRECTORATE	1
 DIRECTOR, PROCUREMENT DIRECTORATE	1
 DIRECTOR, PRODUCT ASSURANCE DIRECTORATE	1

NOTE: PLEASE NOTIFY DIRECTOR, BENET WEAPONS LABORATORY, ATTN: SMCAR-CCB-TL,  
OF ANY ADDRESS CHANGES.

TECHNICAL REPORT EXTERNAL DISTRIBUTION LIST

	<u>NO. OF COPIES</u>		<u>NO. OF COPIES</u>
ASST SEC OF THE ARMY RESEARCH & DEVELOPMENT ATTN: DEP FOR SCI & TECH THE PENTAGON WASHINGTON, D.C. 20315	1	COMMANDER US ARMY AMCCOM ATTN: SMCAR-ESP-L ROCK ISLAND, IL 61299	1
COMMANDER DEFENSE TECHNICAL INFO CENTER ATTN: DTIC-DDA CAMERON STATION ALEXANDRIA, VA 22314	12	COMMANDER ROCK ISLAND ARSENAL ATTN: SMCRI-ENM (MAT SCI DIV) ROCK ISLAND, IL 61299	1
COMMANDER US ARMY MAT DEV & READ COMD ATTN: DRUDE-SG 5001 EISENHOWER AVE ALEXANDRIA, VA 22333	1	DIRECTOR US ARMY INDUSTRIAL BASE ENG ACTV ATTN: DRXIB-M ROCK ISLAND, IL 61299	1
COMMANDER ARMAMENT RES & DEV CTR US ARMY AMCCOM ATTN: SMCAR-FS SMCAR-FSA SMCAR-FSM SMCAR-FSS SMCAR-AEF SMCAR-AES SMCAR-AET-O (PLASTECH) SMCAR-MSI (STINFO) DOVER, NJ 07801	1 1 1 1 1 1 1 2	COMMANDER US ARMY TANK-AUTMV R&D COMD ATTN: TECH LIB - DRSTA-TSL WARREN, MI 48090	1
DIRECTOR BALLISTICS RESEARCH LABORATORY ATTN: AMXBR-TSB-S (STINFO) ABERDEEN PROVING GROUND, MD 21005	1	COMMANDER US ARMY TANK-AUTMV COMD ATTN: DRSTA-RC WARREN, MI 48090	1
MATERIEL SYSTEMS ANALYSIS ACTV ATTN: DRXSY-MP ABERDEEN PROVING GROUND, MD 21005	1	COMMANDER US MILITARY ACADEMY ATTN: CHMN, MECH ENGR DEPT WEST POINT, NY 10996	1
		US ARMY MISSILE COMD REDSTONE SCIENTIFIC INFO CTR ATTN: DOCUMENTS SECT, BLDG. 4484 REDSTONE ARSENAL, AL 35898	2
		COMMANDER US ARMY FGN SCIENCE & TECH CTR ATTN: DRXST-SD 220 7TH STREET, N.E. CHARLOTTESVILLE, VA 22901	1

NOTE: PLEASE NOTIFY COMMANDER, ARMAMENT RESEARCH AND DEVELOPMENT CENTER,  
US ARMY AMCCOM, ATTN: BENET WEAPONS LABORATORY, SMCAR-CCB-TL,  
WATERVLIET, NY 12189-4050, OF ANY ADDRESS CHANGES.

TECHNICAL REPORT EXTERNAL DISTRIBUTION LIST (CONT'D)

	<u>NO. OF COPIES</u>		<u>NO. OF COPIES</u>
COMMANDER US ARMY LABCOM MATERIALS TECHNOLOGY LAB ATTN: SLCMT-IML WATERTOWN, MA 01272	2	DIRECTOR US NAVAL RESEARCH LAB ATTN: DIR, MECH DIV CODE 26-27, (DOC LIB) WASHINGTON, D.C. 20375	1 1
COMMANDER US ARMY RESEARCH OFFICE ATTN: CHIEF, IPO P.O. BOX 12211 RESEARCH TRIANGLE PARK, NC 27709	1	COMMANDER AIR FORCE ARMAMENT LABORATORY ATTN: AFATL/DLJ AFATL/DLJG EGLIN AFB, FL 32542	1 1
COMMANDER US ARMY HARRY DIAMOND LAB ATTN: TECH LIB 2800 POWDER MILL ROAD ADELPHIA, MD 20783	1	METALS & CERAMICS INFO CTR BATTELLE COLUMBUS LAB 505 KING AVENUE COLUMBUS, OH 43201	1
COMMANDER NAVAL SURFACE WEAPONS CTR ATTN: TECHNICAL LIBRARY CODE X212 DAHLGREN, VA 22448	1		

NOTE: PLEASE NOTIFY COMMANDER, ARMAMENT RESEARCH AND DEVELOPMENT CENTER,  
 US ARMY AMCCOM, ATTN: BENET WEAPONS LABORATORY, SMCAR-CCB-TL,  
 WATERVLIET, NY 12189-4050, OF ANY ADDRESS CHANGES.

EWIND

Dtjic

5-86